DOI 10.48612/fpg/38mu-zda7-dpep

© *A. A. Konik*[1,2]*, *A. V. Zimin*[1,2], *O. A. Atadzhanova*[1,3], 2022
© Translation from Russian: *K. A. Kruglova*, 2022

[1]Shirshov Institute of Oceanology, Russian Academy of Sciences, 36 Nakhimovsky Prosp., Moscow, 117997, Russia
[2]St. Petersburg State University, 7–9 Universitetskaya Emb., St. Petersburg, 199034, Russia
[3]Marine Hydrophysical Institute, Russian Academy of Sciences, 2 Kapitanskaya Str., Sevastopol, 299011, Russia
*konikrshu@gmail.com

SPATIAL AND TEMPORAL VARIABILITY OF THE CHARACTERISTICS OF THE RIVER PLUME FRONTAL ZONE IN THE KARA SEA IN THE FIRST TWO DECADES OF THE XXI CENTURY

Received 02.06.2022, Revised 05.11.2022, Accepted 11.11.2022

Abstract

The article is devoted to obtaining long-term physical and geographical characteristics of the River Plume frontal zone as a separate hydrological structure that forms at the boundary of the fresh surface layer of the Ob and Yenisei Rivers. The primary data for identifying the frontal zone are satellite measurements of surface temperature (MODIS Aqua, Suomi NPP-VIIRS), surface salinity (NASA SMAP) and sea level (AVISO) for the period from July to October from 2002 to 2020. The position and characteristics of the River Plume frontal zone were determined using cluster analysis, which was applied for the first time to an integrated set of remote satellite sensing data in this region. The results of the study showed that in the warm period of the year, the average long-term surface temperature gradient of the River Plume frontal zone was 0.08 °C/km, the surface salinity gradient was 0.1 PSU/km, and the area was 155,000 km^2. During the ice-free period of the second decade of the 21st century, the temperature gradient of the frontal zone weakens by 0.04 °C/km, and the area decreases by 100,000 km^2. The correlation analysis showed that the temperature and salinity gradients, as well as the area of the River Plume frontal zone, were determined by the volumes of the river discharge of the Ob and Yenisei and ice parameters in the warm period of the year. The article presents the obtained estimates of the relationship between the characteristics of the frontal zone and the volume of river discharge, ice cover and wind parameters, as well as the value of the atmospheric indices of the Scandinavian oscillation (SCAND).

Keywords: frontal zone, river plume, sea ice, SCAND, Kara Sea

© *А. А. Коник*[1,2]*, *А. В. Зимин*[1,2], *О. А. Атаджанова*[1,3], 2022
© Перевод с русского: *К. А. Круглова*, 2022

[1]Институт океанологии им. П.П. Ширшова РАН, 117997, Россия, Москва, Нахимовский проспект, 36.
[2]Санкт-Петербургский государственный университет,
199034, Университетская наб., 7–9, г. Санкт-Петербург, Россия
[3]Морской гидрофизический институт РАН, 299011, ул. Капитанская, д. 2, г. Севастополь, Россия
*konikrshu@gmail.com

ПРОСТРАНСТВЕННО-ВРЕМЕННАЯ ИЗМЕНЧИВОСТЬ ХАРАКТЕРИСТИК СТОКОВОЙ ФРОНТАЛЬНОЙ ЗОНЫ В КАРСКОМ МОРЕ В ПЕРВЫЕ ДВА ДЕСЯТИЛЕТИЯ XXI ВЕКА

Статья поступила в редакцию 02.06.2022, после доработки 05.11.2022, принята в печать 11.11.2022

Аннотация

Статья посвящена получению многолетних физико-географических характеристик Стоковой фронтальной зоны как отдельной гидрологической структуры, формирующейся на границе поверхностного опресненного слоя рек Оби и Енисея и морских вод в Карском море. В качестве исходных данных для выделения фронтальной зоны в работе выступают спутниковые измерения поверхностной температуры (MODIS Aqua, Suomi NPP-VIIRS), поверхностной солености (NASA SMAP) и уровня моря (AVISO) за период с июля по октябрь с 2002 по 2020 гг. Положение и характеристики Стоковой фронтальной зоны определялись с помощью кластерного анализа,

Ссылка для цитирования: *Коник А.А.*, *Зимин А.В.*, *Атаджанова О.А.* Пространственно-временная изменчивость характеристик стоковой фронтальной зоны в Карском море в первые два десятилетия XXI века // Фундаментальная и прикладная гидрофизика. 2022. Т. 15, № 4. С. 23–41. doi:10.48612/fpg/38mu-zda7-dpep
For citation: *Konik A.A.*, *Zimin A.V.*, *Atadzhanova O.A.* Spatial and Temporal Variability of the Characteristics of the River Plume Frontal Zone in the Kara Sea in the First Two Decades of the XXI Century. *Fundamental and Applied Hydrophysics*. 2022, 15, 4, 23–41. doi:10.48612/fpg/38mu-zda7-dpep

который впервые был применен к обобщённому набору данных дистанционного спутникового зондирования в этом регионе. Установлено, что в теплый период года средний многолетний температурный поверхностный градиент Стоковой фронтальной зоны составляет 0,08 °С/км, градиент поверхностной солености 0,1 PSU/км, а площадь — 155 тыс. км^2. Выявлено, что за безледный период второго десятилетия XXI века градиент температуры фронтальной зоны ослабевает на 0,04 °С/км, а площадь уменьшается на 100 тыс. км^2. Показано, что температурный и соленостный градиенты, а также площадь Стоковой фронтальной зоны определяются объемами речного стока Оби и Енисея и параметрами льдов в теплый период года. Получены оценки связи характеристик фронтальной зоны с объема речного стока, параметрами ледяного покрова и ветра, а также величиной атмосферных индексов Скандинавского колебания.

Ключевые слова: фронтальная зона, речной плюм, морской лед, Скандинавское колебание, Карское море

1. Introduction

The Kara Sea is one of the marginal seas of the Arctic Ocean. The sea is limited from the west by archipelago Novaya Zemlya, from the south by the Siberian coast and from the east by the Laptev Sea (Fig. 1). An important factor in the formation of water masses in the Kara Sea is the continental discharge of large Siberian rivers, the total volume of which is 1,350 km^3/year [1, 2]. The large rivers Ob (430 km^3/year) and Yenisei (650 km^3/year) make the largest contribution to the formation of a large river plume.

In the Kara Sea four main water masses (water types) are distinguished in the surface layer. Barents Sea waters are observed in the west of the Kara Sea [3–5]. The Arctic waters are located in the northern part of the Kara Sea [6]. Kara Sea waters are observed in the south and east of the sea [1–2, 7] and river waters are observed near the confluences of large rivers (the Ob, Yenisei, etc.) [1, 8–9]. River waters, spreading over the water area, form a large freshened surface layer (FSL) (Fig. 1) with an average thickness of about 10 m, which has a significant effect on many physical and biological processes in the Kara Sea [7–11]. The FSL field can reach an area of 200,000–250,000 km^2[7, 12]. Depending on the configuration of the FSL on the sea surface are distinguished “western”, “central”, and “eastern” types of the FSL distribution [1, 10]. The waters in the FSL

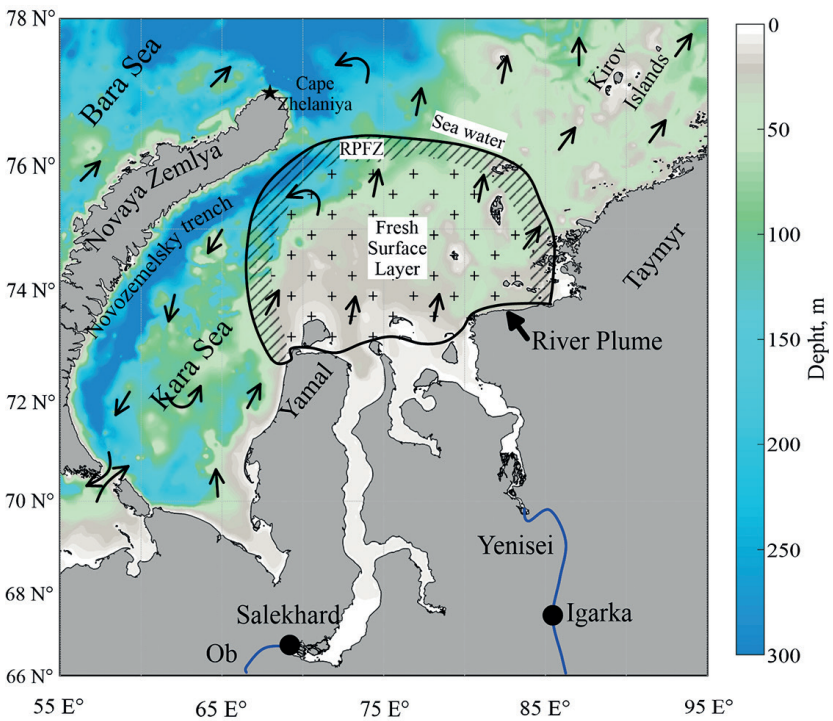

Fig. 1. Geographical objects and the scheme of formation of the river plume frontal zone (RPFZ) in the Kara Sea: black dots show hydrographic posts on the Ob (Salekhard) and Yenisei (Igarka) Rivers, and black arrows show the scheme of middle currents [1] in the Kara Sea

area are relatively warm and vary from 4–5 °C in September to 10 °C in July [1, 3, 7]. As a result of the mixing of sea and river waters, significant fluctuations in salinity are recorded in this area, which can range from 8 to 17 PSU for the period from June to September [7]. It should be noted that such spatial fluctuations are reflected not only in the hydrophysical characteristics of waters, but also in the hydrochemical and biological processes of the sea [11, 13].

The boundary area between the waters of marine and river genesis is characterized by significant instability [8–9]. The interaction between the FSL and sea waters leads to the formation of a barrier or frontal section, where vertical mixing is significantly weakened. According to the classification presented in [14] this boundary can be called the River Plume Frontal Zone (RPFZ). The RPFZ is a zone between river and sea waters characterized by sharp salinity and temperature gradients. In separate studies [11, 14, 15], quantitative estimates of the positions and characteristics of the RPFZ were obtained in certain years. At present, irregular ship salinity measurements are most often used to determine the position of frontal zones in the Kara Sea [7–9]. In most of these studies the entire FSL area is considered and the RPFZ which is its outer boundary remains unexplored. Thus, there are currently no representations about the physical and geographical characteristics of the RPFZ and their variability, which actualizes its study in a changing climate.

It seems that to identify the RPFZ on a regular basis, it is possible to use constantly arriving data from satellite measurements of salinity in combination with temperature and sea level, as was done in work [16]. However, it is currently believed that the errors in determining the characteristics of surface salinity in the cold and fresh waters of the Kara Sea from satellite measurements are very large [17]. At the same time, in order to analyze the large-scale variability of the salinity fields not enough of individual hydrographic stations, which are presented in most studies [7–9]. That's why the use of satellite data to identify the frontal zone requires their validation based on large-scale oceanographic measurements. The results of such validation are given in [12] which shows the possibility of using satellite measurements to determine the physical and geographical characteristics of the frontal zones in the seas of the Arctic.

According to studies [11, 18–19] the formation of the FSL is influenced by many regional factors: the volume of river discharge, the direction and stability of the near-water wind, and the characteristics of sea ice conditions in the water area. As noted in [2, 20] the global atmospheric circulation over the Kara Sea makes a significant contribution to the formation and variability of its hydrophysical characteristics. Accordingly, the spatial dynamics and characteristics of the RPFZ are formed under the influence of regional and global processes of interaction between the ocean and the atmosphere. However, until now separate comprehensive description of the long-term variability of the RPFZ parameters in the Kara Sea and the factors influencing it has not been carried out.

Even in the presence of constantly incoming satellite data the lack of information about the RPFZ is associated with the problem of choosing a methodological tool for studying frontal zones in the Arctic region [2, 4, 9]. According to the concept presented in [14], the frontal zone is the area where the horizontal gradient of the characteristic significantly (by an order of magnitude) exceeds its background distribution. In the seas of the Arctic region, as a rule, there are no significant gradients on the surface [21, 22]. For this reason, it is difficult to determine the spatial dynamics and characteristics of the frontal zones. Analysis of hydrological fields of several characteristics will increase the accuracy of determining the position of the frontal zone. One of the approaches that allows to identify areas with large gradients of different characteristics is the use of cluster analysis.

Thus, the purpose of this study is to study the spatiotemporal variability of the RPFZ characteristics in the Kara Sea for the period from 2002 to 2020 and analysis of the degree of its connection with processes of different scales.

2. Data

To determine the dynamics and parameters of the RPFZ, monthly average satellite measurements of temperature, salinity and sea level were used from July to October from 2002 to 2020, presented in Table 1.

To identify the thermal characteristics of the RPFZ, we used sea surface temperature (SST) data from high-resolution infrared radiometers MODIS Aqua and Suomi NPP VIIRS with a spatial step of 0.05° [23]. The use of NASA SMAP radiometric data with a spatial resolution of 1/4° made it possible to determine the characteristics of the sea surface salinity (SSS) of the RPFZ [24]. Level fluctuations in the RPFZ were analyzed using absolute dynamic topography (ADT) data from the AVISO data set with a spatial step of 1/4° [25].

Table 1

Types and parameters of data

Sensor/ Data set	Data type	Time	Level
MODIS	SST	07.2002–10.2011	L3
NPP VIIRS		07.2012–10.2020	L3
SMAP	SSS	07.2015–10.2020	L3
Aviso	ADT	07.2002–10.2020	L4
Arctic rivers	River discharge	05.2002–10.2020	-
CMEMS	Wind	07.2002–10.2020	L4
AMSR-E	Sea ice	07.2002–10.2011	L3
AMSR-2		07.2012–10.2020	L3

To analyze the influence of regional processes on the dynamics and parameters of the RPFZ, we used data on river discharge obtained at the hydroposts closest to the Kara Sea on the Ob in Salekhard and the Yenisei in Igarka (Fig. 1). In addition, 6-hour surface wind speed data (east and north components) were used with a spatial resolution of 1/4° of the data set SIW-IFREMER-BREST-FR obtained from the Copernicus Marine Environmental Monitoring Service[1]. Sea ice conditions (area and state in the study area) were described using data from the AMSR-E and AMSR-2 radiometers prepared by the University of Bremen [26].

Analysis of influence of global atmospheric transport over Northern Eurasia on the change in the parameters of the RPFZ in the Kara Sea was carried out using atmospheric circulation indices obtained from the site Climate Prediction Center[2]. The study used the Scandinavian (SCAND) and Polar (POL) oscillation indices [27]. The SCAND index shows the change in atmospheric pressure over Scandinavia and, at positive values, is characterized by an increase in the blocking of zonal air mass transfers, and at negative values, their weakening over the Scandinavia peninsula [28]. The POL index describes the atmospheric pressure variability between the Arctic and Eurasia [28–29]. Positive values of the index characterize an increase in the intensity of cyclonic activity in the Arctic and an increase in meridional transfers, while negative values characterize a weakening of cyclones and transfers.

3. Methods

3.1. Determination of the RPFZ waters on the surface of the Kara Sea

The SST, SSS, and ADT data were loaded for determining the spatial position and quantitative estimates of the frontal zones. If field data were missing or the number of gaps, for example, due to a large amount of sea ice on the surface or cloud cover, exceeded 20 %, then they were not used further.

The main criterion for determining the frontal zone is an increased gradient of the characteristics of hydrological fields, the value of which is two times higher than the background gradient of the Kara Sea [21–22]. Therefore, further, we calculated the horizontal gradients of temperature and salinity according to the method presented in [22].

Then regular two-dimensional region was created in software MATLAB using the function «griddata». The coordinates of the grid boundaries corresponded to the central part of the Kara Sea: 69–78°N and 55–95°E. The step of grid nodes was 1/4°. Linear interpolation of satellite data of SST, SSS, their gradients and ADT was performed on the constructed grid. The obtained data array was used to identify the surface water masses of the Kara Sea by cluster analysis using the Statistica 10.0 software package. The main task of the analysis was to split the data into homogeneous groups that are stable in time and location.

[1] CMEMS, https://doi.org/10.48670/moi-00185 (accessed 01.10.2022)

[2] https://www.cpc.ncep.noaa.gov (accessed 04.10.2022)

All data in the combined matrix was standardized: each characteristic (SST, SSS, their gradients and ADT) was divided by its maximum value before starting the calculation of clusters. At the first stage, a hierarchical clustering algorithm based on the Ward method with the Euclidean metric was used for exploratory analysis. Using the obtained dendrograms for different months and years, a preliminary assessment was made of the optimal number of classes and subclasses that can correspond to different types of water. The number of classes obtained using Ward's method was used as a priori constraints for the final partitioning of the data using the interactive k-means method.

Based on the results of the cluster analysis, monthly maps of the distribution of the identified class positions were built with an emphasis on the RPFZ. The resulting maps of the positions of the main water classes were analyzed for each individual month. For the class corresponding to the RPFZ, at monthly and annual intervals, the average values of the zone characteristics were calculated: SST, SSS, their gradients, ADT and area.

3.2. Methods for analyzing the impact of regional and global processes on the characteristics of the RPFZ

Cross-correlation analysis was used to determine the degree of connection between regional and global processes and the RPFZ characteristics.

Comparison of the characteristics of the frontal zone with data on river discharge, wind, sea ice cover area and state were carried out on a monthly interval with a shift of up to 12 months. For these indices of atmospheric circulation, a correlation analysis was carried out with average seasonal estimates of the characteristics of the frontal zone in the time interval with a shift from 0 to 3 seasons. The obtained coefficients were tested using Student's t-test. The paper describes only the coefficients significant at the 95 % level.

4. Results and discussion

4.1. Results of cluster analysis

The prepared data for August 2019 were used as an example to determine and obtain the characteristics of the RPFZ. The results of clustering by the Ward algorithm are shown in Figure 2, *a*. On the dendrogram, two main classes were clearly distinguished, which suggests the presence of significant differences between the characteristics of the waters. These classes can be interpreted as marine and freshened waters. By reducing the threshold distance by an average of three times, each of the classes can be divided into two subclasses. The class identified as marine waters was more clearly divided into subclasses than freshened. From physical

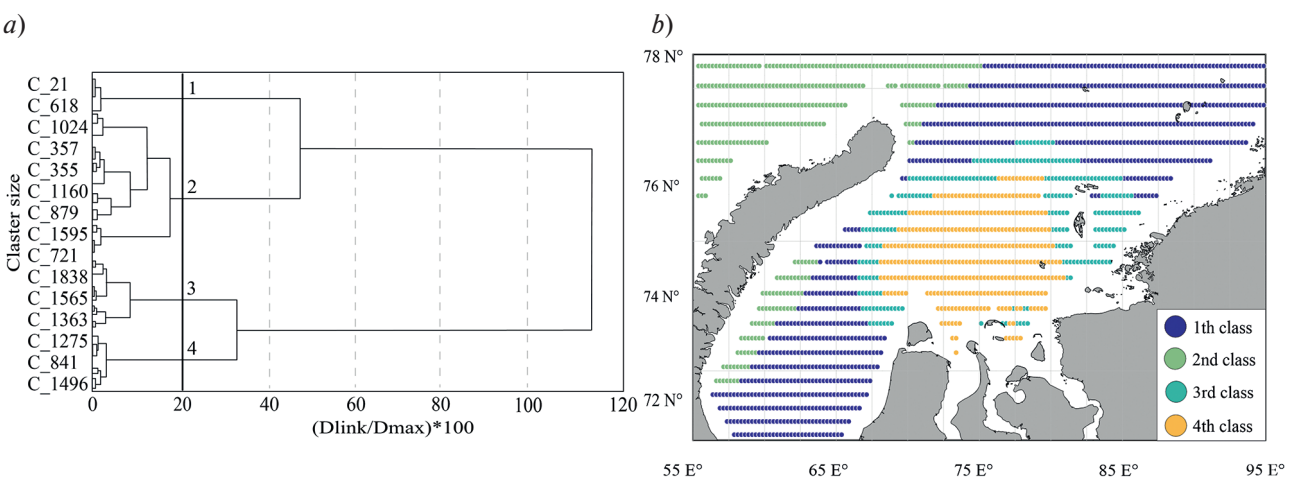

Fig. 2. The results of cluster analysis based on satellite data in August 2019 in Kara Sea: *a* — dendrogram obtained by Ward's method. Black vertical lines and numbers indicate the main classes of waters; *b* — is the classification obtained by the k-means method: class 1 (blue) — is the Kara waters, class 2 (green) — Barents waters, class 3 (turquoise) — is the outer boundary of the FSL — RPFZ, class 4 (orange) — is the inner part of the FSL

considerations, it is known [1, 2, 8, 11] that sea waters in this area are divided into Barents Sea waters and Kara Sea waters. River waters, as a rule, are represented as a single class [7], which is quite logical, if you set a formal level of division into classes that is the same as sea waters (Fig. 2, *a*). However, the presented dendrogram shows that the class of river waters also had a clear division into two subclasses, which will be referred to as the waters of the inner part of the FSL and the waters of the RPFZ. In the studies [7, 9] often noted the presence of frontal sections in the FSL area, the water characteristics in which differ from the bulk of the waters of the lens of freshened waters. Accordingly, the results of cluster analysis by the Ward method allow us to conclude that in river waters, as well as in sea waters, there is a clear division into waters with different characteristics. As a result, in this region, the most optimal from a physical and statistical point of view will be the allocation of four classes of water. Further detailed division into classes is not advisable.

The resulting number of classes was used in the k-means clustering method, the results of which are shown in Figure 2, *b*. Quantitative estimates of the resulting clustering are presented in Table 2. It can be seen from this table that the classification made allows us to quite clearly correlate the obtained classes with waters of different genesis that are observed in the Kara Sea.

According to [1–3, 5–6], the Kara Sea waters are located near the Yamal Peninsula and archipelago Novaya Zemlya in the west, as well as in the north and east of the Kara Sea near the Taimyr Peninsula. The spatial position of class 1 (Fig. 2, *b*) completely coincides with the description of the climatic position of this water mass, the average temperature of which is 6–8 °C, and salinity is 24–28 PSU [1, 2, 7]. It should be taken into account that the Kara Sea waters constantly interact with other types of waters, which affects its hydrological characteristics [1, 3]. In this regard, there may be differences between the received and climatic thermohaline estimates, especially in salinity characteristics. However, the estimates of surface temperatures and salinity are close to the indices corresponding to the Kara Sea waters.

The Barents Sea waters enter the Kara Sea from the west, north of Cape Zhelaniya, and spread to the east through the Novaya Zemlya straits in a southern way [3–5]. The climatic description of the position is partially similar to the location of the second class (Fig. 2, *b*). This water mass is characterized by a relatively high temperature in the southwestern part of the Kara Sea (up to 8–10 °C) and a low temperature in the northeast of the sea (4–5 °C) [4]. The average salinity of the waters is 30–32 PSU, which is much higher in comparison with other water masses in this region [4–5]. Thus, the average long-term estimates of the indices of the Barents Sea waters coincide with the quantitative estimates of the 2nd class obtained in the course of the clustering.

The position of waters of classes 3 and 4 shown in this example (Fig. 2, *b*) corresponds with the "central" type of distribution of waters in the FSL, which is quite common [10]. FSL, according to [7], is characterized by low salinity (~15 PSU) and high temperatures (~8 °C), which is also similar to the classes 3 and 4 estimates (Table 2). However, earlier expeditionary studies [7–9] and satellite data analysis [10] note the presence of several separate frontal sections on the «western», «eastern», and «central» boundaries of the FSL. This makes it

Table 2

Quantitative estimates of the characteristics of SST, SSS, ADT and their gradients based on the results of clustering in August 2019: $\bar{T}$ — SST; $\nabla\bar{T}$ — SST gradient; $\bar{H}$ — ADT; $\bar{S}$ — SSS; $\nabla\bar{S}$ — SSS gradient; *s* — class area

Parameters	1 class	2 class	3 class	4 class
$\bar{T}$, °C	5.9	4.7	7.8	8.6
$\nabla\bar{T}$, °C/km	0.05	0.04	0.06	0.04
$\bar{H}$, cm	–6.9	–20.4	1.6	7.5
$\bar{S}$, PSU	28.0	32.6	19.5	12.8
$\nabla\bar{S}$, PSU/km	0.07	0.06	0.11	0.08
$s*10^3$, km^2	378	168	96	138

possible to assume that class 3, which differs in the maximum value of the SST and SSS gradients, belongs to the frontal sections identified earlier at the outer boundary of the FSL. The fourth class, characterized by reduced salinity and SSS gradients (Table 2), is the internal of the FSL waters (Fig. 2, *b*).

The position of waters of the 3rd class, obtained from the results of clustering, is similar to the study [8–9], where the positions of fronts were considered of different genesis associated with the FSL region. The waters of this class have an average salinity of 19 PSU and occupy an intermediate position between the Kara Sea waters (28 PSU) and the internal lens of the FSL water (12 PSU). Class 3 has maximum SST and SSS gradients, which, according to the classification [14], confirms its identification with the frontal zone. An analysis of the results obtained allows us to attribute this class to the waters of the RPFZ, which are formed at the boundary between the Kara Sea waters (class 1) and the internal lens of the FSL water (class 4).

Thus, within the framework of the conducted clustering and its analysis, it was possible to distinguish four types of waters: the Barents Sea, the Kara Sea, the RPFZ, and the internal lens of the FSL.

4.2. Average long-term variability of the RPFZ

The implementation of the cluster analysis made it possible to obtain long-term quantitative estimates of the variability of the characteristics of the RPFZ during the ice-free period. Table 3 presents the averaged long-term parameters for the warm season by months (July, August, September, October) for the period from 2002 to 2020, as well as the average characteristics of the RPFZ for the entire study period.

The average long-term SST estimates for each month reflect the general annual course with a maximum in August. The magnitude of the SST and SSS gradients during the warm season is on average two times higher than the background gradients of the Kara Sea [1], the maximum of the gradients is recorded in July. The minimum ADT values are observed in July, and the maximum values are reached in October. The area of the surface the RPFZ during the warm season increases, reaches a maximum in September and then declines. The zone of elevated gradients associated with the RPFZ occupies up to 15 % of the area of the Kara Sea. It should be noted that for October it was not possible to obtain average long-term estimates of the salinity of the RPFZ due to the lack of data in most of the years under consideration.

The analysis of spatial variability showed the presence of a seasonal variation in the dynamics of the RPFZ. In July, the RPFZ is located in the central part of the sea and has a rather narrow distribution area. The northern boundary of the zone is located at the archipelago Novaya Zemlya, and the southern borders at the Yamal and Taimyr Peninsulas. In August, the area of the zone increases significantly, and its northern boundary shifts closer to the Siberian coast. The area of the frontal zone increases especially strongly in the east. September is characterized by a complete shift of the RPFZ zone to the east. The area of the zone does not decrease much, however, the RPFZ extends to the east up to 95 °E. In October, the area of the RPFZ decreases significantly, and the zone itself is completely located along the eastern part of the Siberian coast. It is important to note that the western part of the RPFZ in all months of the study is located near the Yamal Peninsula.

Table 3

Average long — term monthly and average for the entire period of the study quantitative characteristics of the RPFZ: $\bar{T}$ — SST; $\nabla\bar{T}$ — SST gradient; $\bar{H}$ — ADT; $\bar{S}$ — SSS; $\nabla\bar{S}$ — SSS gradient; s — area of the RPFZ

Month	$\bar{T}$, °C	$\nabla\bar{T}$, °C/km	$\bar{H}$, cm	$\bar{S}$, PSU	$\nabla\bar{S}$, PSU/km	$s*10^3$, km^2
July	5.4	0.10	–0.8	18.6	0.14	130
August	6.3	0.06	1.2	22.6	0.10	159
September	4.3	0.08	5.9	25.7	0.10	175
October	2.8	0.08	9.3	—	0.06	157
Average	4.7	0.08	3.9	22.3	0.10	155

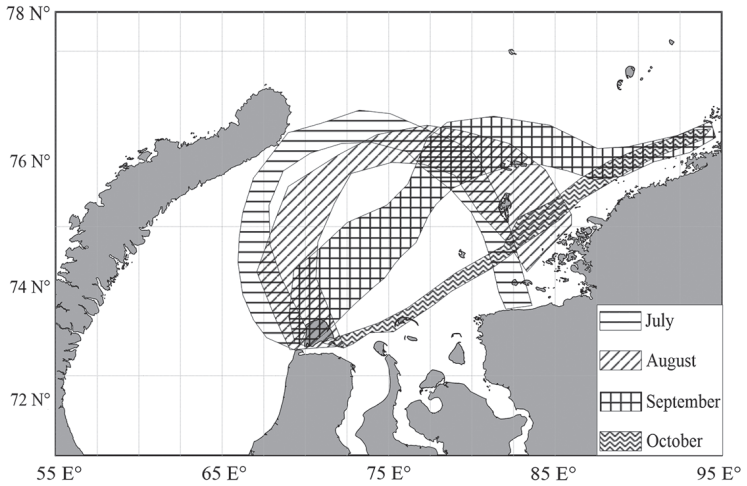

Fig. 3. Average RPFZ positions from July to October for the period from 2002 to 2020

4.3. Interannual variability of the RPFZ

The variability of the temperature characteristics and its gradient in the RPFZ for the entire period under consideration is shown in Figure 4. It can be seen that from 2002 to 2020 the SST in the RPFZ ranges from 1 °C in October to 9.9 °C in August. Most often, the maximum values of surface temperature are recorded in August, the minimum SST values are observed in October. Between 2002 and 2010 the SST parameters in each season correspond to the annual temperature variation in the Kara Sea: the minimum values are observed in autumn, and the maximum values are observed in summer. However, from 2011 to 2020 pronounced positive and negative anomalies of SST characteristics are observed in the RPFZ. For example, in August 2014 and 2018 The SST is 3.1 °C, which is almost two times lower than the average estimates obtained over the entire study period (Table 3). At the same time, in the last five years there has been a positive trend of surface temperature in the RPFZ, the magnitude of which is influenced by highs in August 2015 ($\overline{T}$ = 8.8 °C) and 2020 ($\overline{T}$ = 9.9 °C).

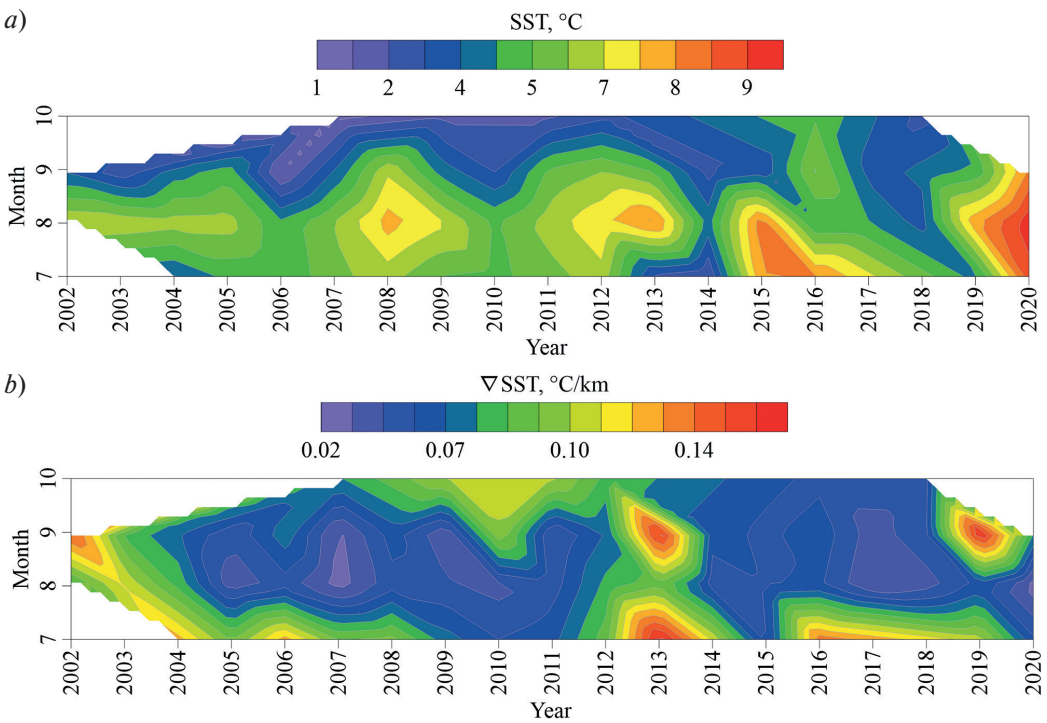

Fig. 4. The SST parameters (*a*) and the SST gradients (*b*) in the RPFZ for the period from July to October 2002–2020

The magnitude of the SST gradient in the RPFZ for the period from 2002 to 2020 characterized by significant heterogeneity. On average, the temperature gradient in the RPFZ varies from 0.03 °C/km in August 2020 to 0.17 °C/km in July 2013. The long-term variability of the SST gradient showed that maximums are most common in July and September, while the minimums are in August and October. Thus, the value of the gradient for an individual month may differ from the average long-term value of the RPFZ gradient by more than two times (Table 3). In some months, there is an inverse relationship between the parameters of the SST gradient and the values of the surface water temperature: in July 2013 ($\overline{T}$ = 2.9 °C; $\nabla\overline{T}$ = 0.17 °C/km), August 2015 ($\overline{T}$ = 8.5 °C; $\nabla\overline{T}$ = 0.05 °C/km) and September 2019 ($\overline{T}$ = 4.5 °C; $\nabla\overline{T}$ = 0.17 °C/km). It is also important to note that in the second decade of the 21st century, the temperature gradient decreased on average by 0.04 °C/km.

Due to the relatively late start of operation of the NASA SMAP satellite compared to other systems (Table 1), data on surface salinity in the RPFZ are available only for the period from 2015 to 2020 (Fig. 5, *a*). The characteristics of the SSS change from a minimum in July ($\overline{S}$ = 17 PSU) to a maximum in September ($\overline{S}$ = 29 PSU). In July, freshened waters are observed in most years, the surface salinity of which does not exceed 17–19 PSU. In August, a gradual increase in SSS values begins, and the value reaches its maximum values in September. In general, there is a gradual decrease in SSS in the RPFZ by an average of 3–5 PSU. However, there are no significant deviations in the obtained interannual estimates when compared with the average values of the SSS in the RPFZ (Table 3).

Fluctuations in SSS gradients (Fig. 5, *b*) over the study period range from 0.08 PSU/km in September to 0.19 PSU/km in July 2016. The maximum variability of surface salinity gradients is observed in August and September. A relatively stable gradient value is observed in July and October. August 2015 and August 2018 stand out against the background of general variability by anomalously low values of the SSS gradient ($\Delta\overline{S}$ = 0.09 PSU/km). This negative anomaly is reflected in the characteristics of surface temperature and SST gradients (Fig. 5). The heterogeneity of the parameters of the surface salinity gradient complicates its comparison with the average value presented in Section 4.2 (Table 3).

The variability of ADT characteristics in the RPFZ is shown in Fig. 6, *a*. The minimum ADT value was registered in August 2004 ($\overline{H}$ = –7.1 cm), and the maximum in October 2007 ($\overline{H}$ = 18.1 cm). An intra-seasonal course is observed, which is characterized by minima in the summer months and maxima in the autumn. The obtained calculations show the presence of negative (2004, 2008, 2015, 2017) and positive (2013, 2016) ADT anomalies. However, the positive average level for the period from 2002 to 2020 (Table 3) is comparable with the results of the interannual variability of the ADT parameters.

The change in the RPFZ area based on the results of the analysis is shown in Fig. 6, *b*. The minimum value of the RPFZ area is observed in July 2016 (s = 55,000 km^2), and the maximum in September 2007 (s = 340,000 km^2). It is important to note that the intra-seasonal course of the RPFZ area is characterized by great heterogeneity. For example, in 2011, the monthly value of the area practically did not change and averaged 200,000–210,000 km^2. Concurrently, in 2009, for four months, the area varied from 50 000 to 160 000 km^2. An analysis of long-term variability shows that in the first decade of the 21st century, on average, the area was 4 times larger compared to the period of 2012–2020. A turning point in the variability of characteristics occurred in 2012, when the area decreased from 220,000 to 89,000 km^2. Between 2012 and 2020 there is a negative trend, the area of the RPFZ is significantly reduced.

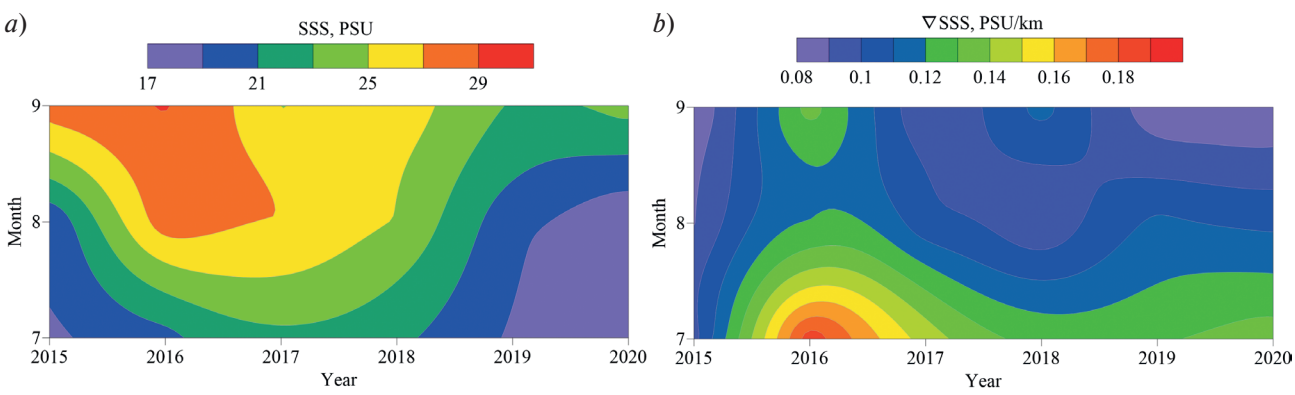

Fig. 5. The parameters of the SSS (*a*) and the SSS gradients (*b*) in the RPFZ for the period from July to September 2002–2020

The analysis of intra-seasonal and inter-annual spatial variability revealed several types of spatial distribution of the RPFZ and the inner region of the FSL, which are shown in Fig. 7.

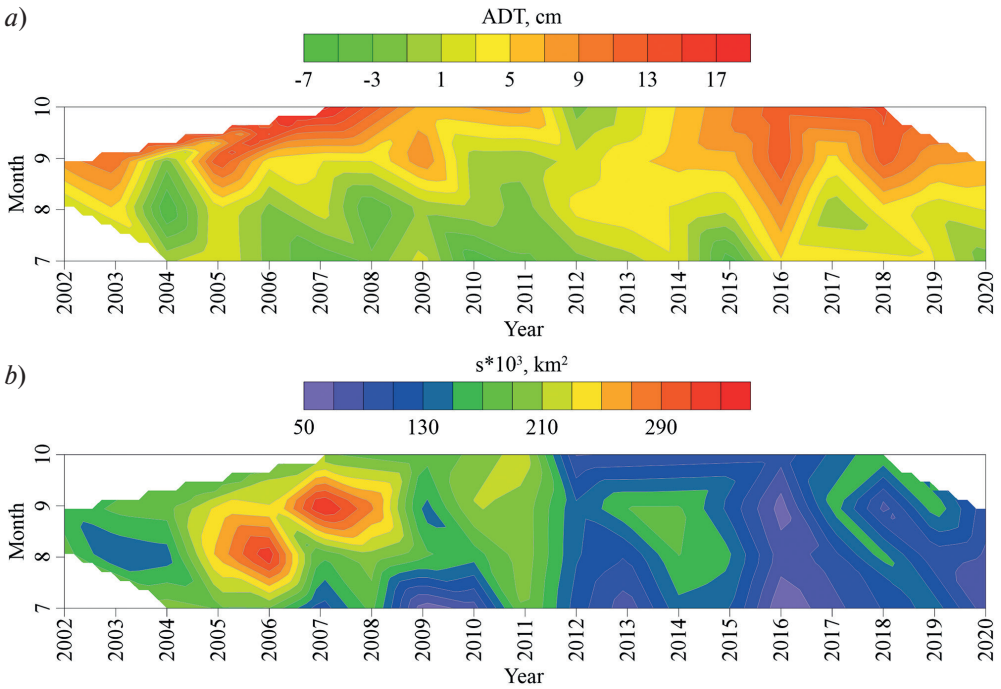

Fig. 6. The parameters of the ADT (*a*) and the area (*b*) of the RPFZ for the period from July to October 2002–2020

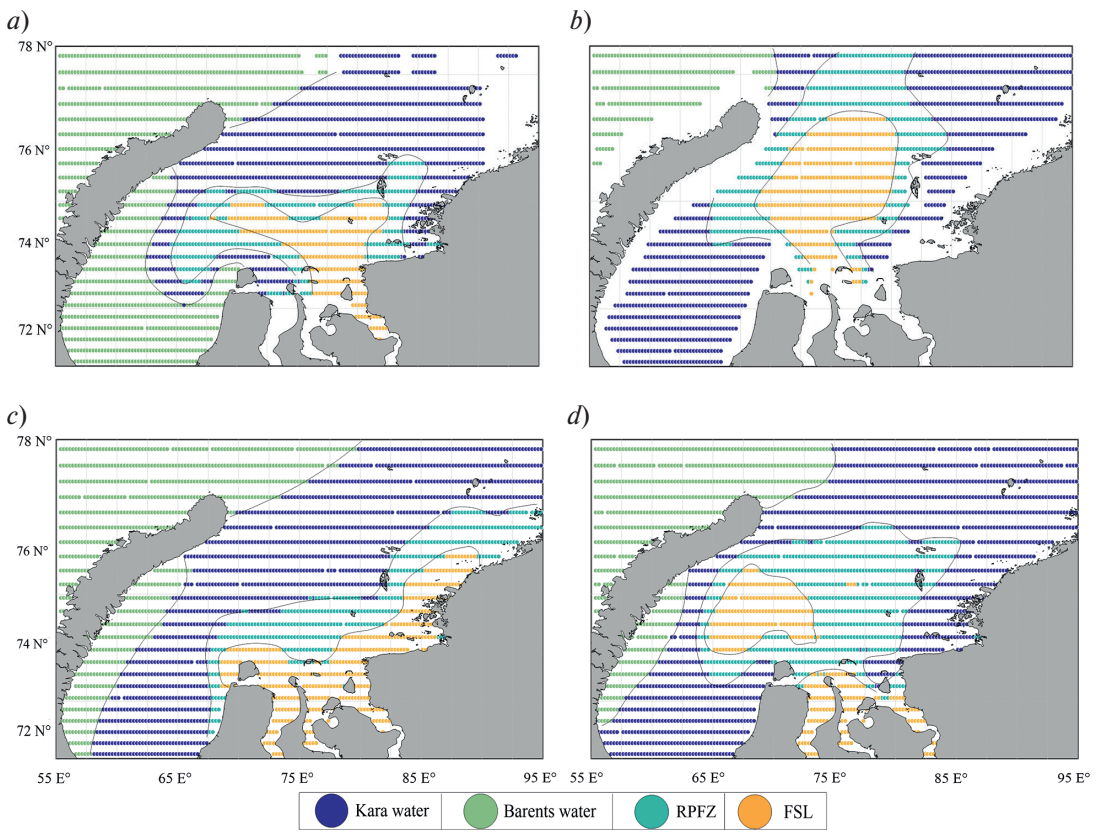

Fig. 7. Types of spatial variability of the main water masses and RPFZ (3th class) according to the results of cluster analysis: *a* — western type on the example of July 2007; *b* — central type on the example of August 2015; *c* — eastern type on the example of September 2009; *d* — atypical type on the example of August 2011

The "western" type (Fig. 7, *a*) is characterized by the position of the RPFZ in the region of 55–65 °E. at the western part of the archipelago Novaya Zemlya. It can be seen that the inner part of the FSL also stands out to a greater extent in the west, and the Barents Sea waters almost completely occupy the southwestern part of the sea. The "central" type (Fig. 7, *b*) is characterized by the location of the RPFZ in the area between 65–85 °E. The western and eastern border of the RPFZ near of the Ob and Yenisei rivers is thin, and increases closer to the center. The inner area of the FSL is located in the RPFZ and is connected to the estuarine sections of the rivers. With this position of the frontal zone, the predominance of the Kara Sea waters on the sea surface is also observed. The "eastern" type (Fig. 7, *c*) of distribution is characterized by the location of the RPFZ along the Siberian coast: from the Yamal Peninsula to the eastern tip of the Taimyr Peninsula. With a relatively large propagation length (from 65 to 95° E), the RPFZ is rather narrow. The inner region of the FSL turns out to be pressed against the mouth sections of the rivers and the coast. The "atypical" type (Fig. 7, *d*) of the RPFZ is observed when the frontal zone completely surrounds the inner area of the FSL, which is divided into a number of isolated sections. The main feature of this type of distribution is that the lens of the inner region of the FSL is detached from the mouth sections of the rivers. With such a distribution, the RPFZ is located on the periphery of the internal region of the FSL and occupies a large area.

4.4. The influence of river discharge and sea ice cover on variability of the RPFZ parameters

Seasonal variability of characteristics. The most important regional feature of the Kara Sea, which affects the formation of the FSL and the RPFZ, is the variability of the river discharge of the large Siberian rivers Ob and Yenisei [1–2, 30]. In addition, the characteristics of the surface water layer of the sea as a whole are influenced by the features of sea ice conditions [1, 31]. Average long-term estimates of these processes are presented in Table 4.

The average long-term variability of the total river discharge of the Ob and Yenisei is characterized by a pronounced maximum in June (~100,000 m^3/s) and a minimum in October (~25,000 m^3/s), which is associated with the onset of spring floods and autumn low-water periods of the rivers [30]. In May, the maximum area and state of the sea ice cover is also observed, which sharply begins to decrease in June. Further, there is a gradual decrease in the discharge of rivers in the middle of summer and the almost complete liberation of the central part of the Kara Sea from sea ice. The minimum level of discharge for the warm season is observed in the autumn period. The minimum area and state of the sea ice cover is observed in September, after which their gradual increase is noted in October.

Comparison of the average long-term parameters of the RPFZ (Table 3) and river discharge showed that in July, due to the impact of a large volume of river waters, the maximums of SST and SSS gradients and the minimums of the SSS and ADT values are observed in the RPFZ. Concurrently, the area of the RPFZ is minimal in this month, which is associated with the processes of intensification of mixing against the background of increased river discharge and insufficient radiation heating. The decrease in the surface temperature and salinity gradient and the increase in SST in the RPFZ in August are probably associated with the minimization of inhomogeneous temperature and salinity zones due to a significant reduction in the area of influence of sea ice melting and an increase in the influx of solar radiation [1, 7]. A decrease in the volume of warm river waters of the Ob and Yenisei in August leads to stabilization of the frontal zone and an increase in the values of SSS, ADT in the RPFZ, as well as an increase in its area. In September, a sharp decrease in the volume of river discharge

Table 4

Average long-term estimates of the river discharge of the Ob and Yenisei, the area of the ice cover and its concentration from May to October for 2002–2020

Month	Discharge of the Ob, m^3/s	Discharge of the Yenisei, m^3/s	Sea ice area, km^2*10^3	Sea ice state,%
May	19465	36572	532	87
June	32307	66095	332	60
July	21166	49959	188	23
August	16548	37928	25	7
September	13612	31639	13	3
October	10797	15041	204	22

and the absence of the effect of sea ice melting in this area determine the continuing increase in the values of ADT, SSS, and the area of the RPFZ. The magnitude of the SST gradient increases and the values of the surface temperature in the RPFZ decrease. This is probably due to a decrease in the influx of solar radiation and the onset of cooling processes [1] in the Kara Sea. At the same time, the magnitude of the SSS gradient in the RPFZ does not change compared to the previous months. In October, the maximum ADT value in the RPFZ is noted, which is associated with the beginning of the autumn low-water period for the Ob and Yenisei rivers [30]. As a result of intensive cooling of the entire water column of the Kara Sea, formed by negative air temperatures [3], the parameters of the SST and the area of the RPFZ are significantly reduced. However, due to the increase in the area and state of sea ice [1, 3], there are more and more inhomogeneities arise in the fields of thermohaline characteristic, which leads to a relatively large value of the temperature gradient of the RPFZ.

Interannual variability of characteristics. Estimates of river discharge characteristics, area and state of sea ice cover by years are presented in Fig. 8. Nevertheless, positive ones are observed (2002–61 000 m^3/s; 2007–58 000 m^3/s; 2014–56 000 m^3/s; 2015–57 000 m^3/s) and negative anomalies (2012–35 000 m^3/s) of the total discharge. The area and state of the sea ice cover have a general negative trend, which is especially pronounced in some years (2011–136 000 km^2, 23 %; 2012–133 000 km^2, 26 %; 2016–153 000 km^2, 20 %, 2020–120 000 km^2, 19 %). It is important to note that in some years (from 2011 to 2014; from 2014 to 2016), the total river discharge and the area with sea ice state change quasi-synchronously.

Comparison of the interannual parameters of discharge and sea ice with the characteristics of the RPFZ showed that the overall increase in the surface temperature of the RPFZ (Fig. 4, *a*) over the period from 2002 to 2020 is formed against the background of negative values of the area, state of the sea ice cover and river discharge. It should be noted that the relatively low SST in the RPFZ (4.7 °C) in 2010 coincides with small values of the area and state of the sea ice cover. A sharp increase in the volume of river discharge of the Ob and Yenisei rivers, the area and state of the sea ice cover coincides in time with the minimum SST values in the RPFZ in 2011 and 2018. The increase in SST values in the RPFZ in 2016, 2019–2020 corresponds with a decrease in sea ice state and sea ice area. In this way, the large variations in the surface temperature of the RPFZ in the second decade of the XXI century with declining sea ice area and sea ice state, reflect global climate change in the Arctic [32].

The large SST gradient in the RPFZ, recorded in 2002 and 2013, coincides with the year of increased river discharge against the background of increased values of sea ice state. An increase in the temperature gradient in these years is likely due to an increase in temperature contrasts between a large volume of warm river water and ice-cooled sea water. Small values of the SST gradient in the RPFZ occur against the background of a small area and sea ice state, which reduces the temperature contrast between sea and river waters.

The change in surface salinity in the RPFZ generally corresponds with the change in the river discharge of the Ob and Yenisei: a low salinity value is noted at the end of the spring flood, and an increase at the beginning of the autumn low-water [30]. The same processes are also reflected in the magnitude of the SSS gradient in the RPFZ.

Long-term level fluctuations (Fig. 6, *a*) in the period from 2002 to 2010 are generally stable, which is associated with a small amplitude of river discharge variability in this period. A significant decrease in the volume of the river waters of the Ob and Yenisei in 2011 is reflected in the observed positive ADT anomaly.

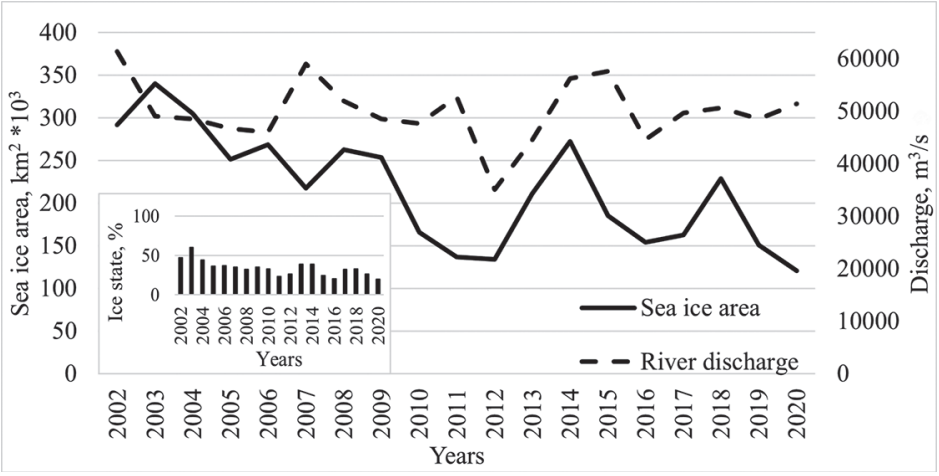

Fig. 8. Interannual estimates (2002–2020) of river discharge Ob and Yenisei, sea ice cover area and its state in the study area

The maximum values of the area of the RPFZ in the first decade of the 21st century (2006, 2007) correspond with the large volumes of the river discharge of the Ob and Yenisei, which increase the area of distribution of river waters in the Kara Sea. Between 2011 and 2020 the size of the area decreases significantly, but the amplitude of its variability increases. The small value of the area of the RPFZ in 2012 and 2016 is noted at the minimum values of river discharge and sea ice characteristics. Probably, the homogenization of waters that occurs against the background of relatively stable SST and SSS values leads to the minimization of heterogeneous zones, and, as a result, the area of the RPFZ.

Correlation analysis showed that the volume of river discharge of the Yenisei has a significant correlation coefficient for July ($r = 0.61$) and August ($r = 0.51$) with the values of the RPFZ area in September. Probably, large volumes of river discharge in the first months of summer form a significant area of the FSL, which then intensively mixes with sea waters in September, which is reflected in the increase in the area of the RPFZ in subsequent months. The area and state of sea ice for October of the previous year correlates with the July temperature values ($r = -0.72$) and the August values of the SST gradient ($r = 0.58$) in the RPFZ. A possible reason for this relationship is the fact that the area of sea ice formed in October is an indicator of the heat reserve of sea waters [31] formed during the warm season. As a result, the value of the heat reserve affects the decrease in sea temperature during the formation of the frontal zone, which, as the surface layer warms up, is reflected in the intensification of the temperature gradient of the RPFZ.

4.5. The influence of wind on the variability of the RPFZ characteristics

One of the key factors influencing the surface dynamics of the waters of the Kara Sea is the wind effect [1, 3]. To analyze the relationship between wind dynamics and the position of the frontal zone, composite maps were built, shown in Fig. 9.

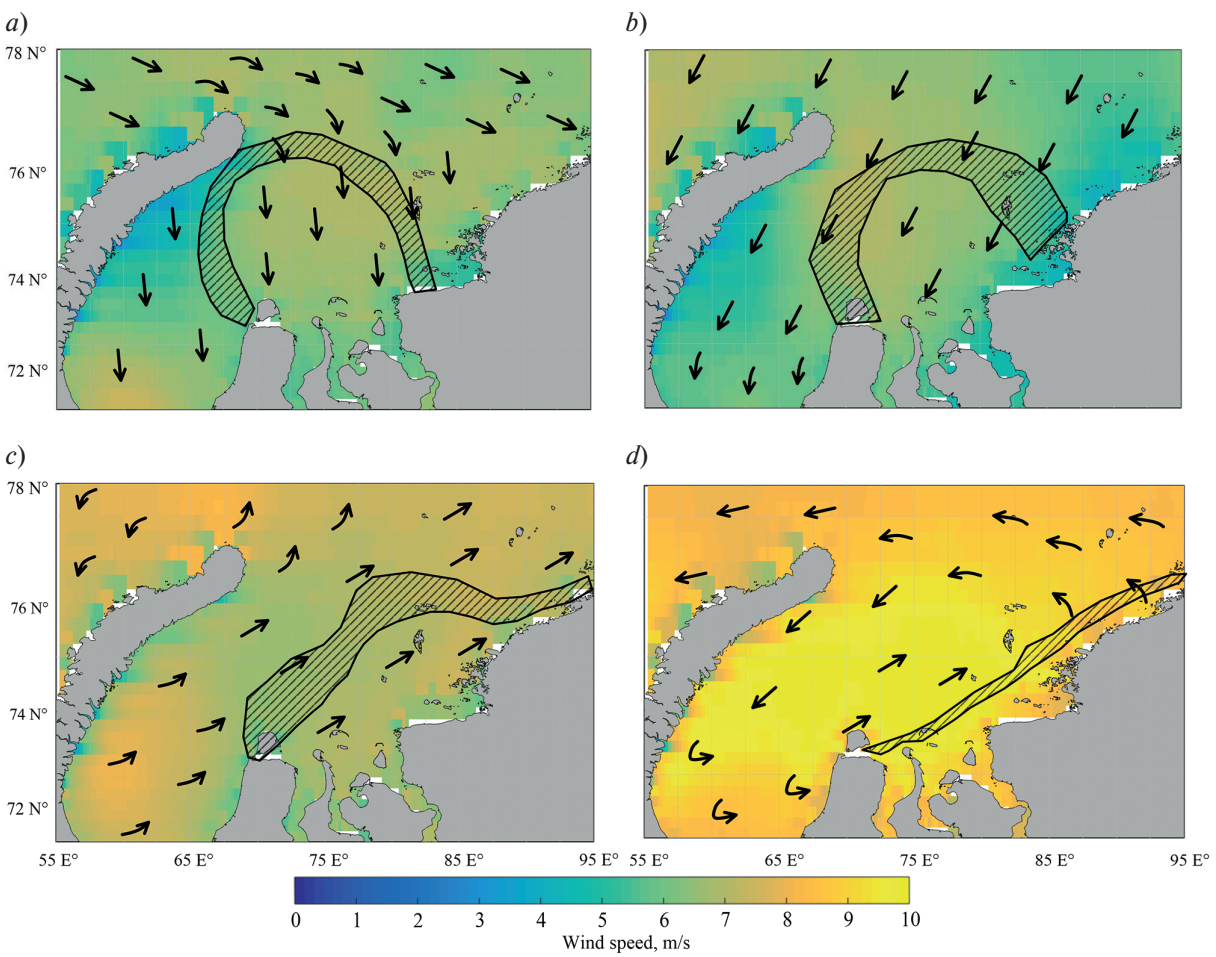

Fig. 9. Composite map of wind speed and direction over the Kara Sea and RPFZ positions according to the average multiyear data of 2002–2020: *a* — July, *b* — August, *c* — September, *d* — October

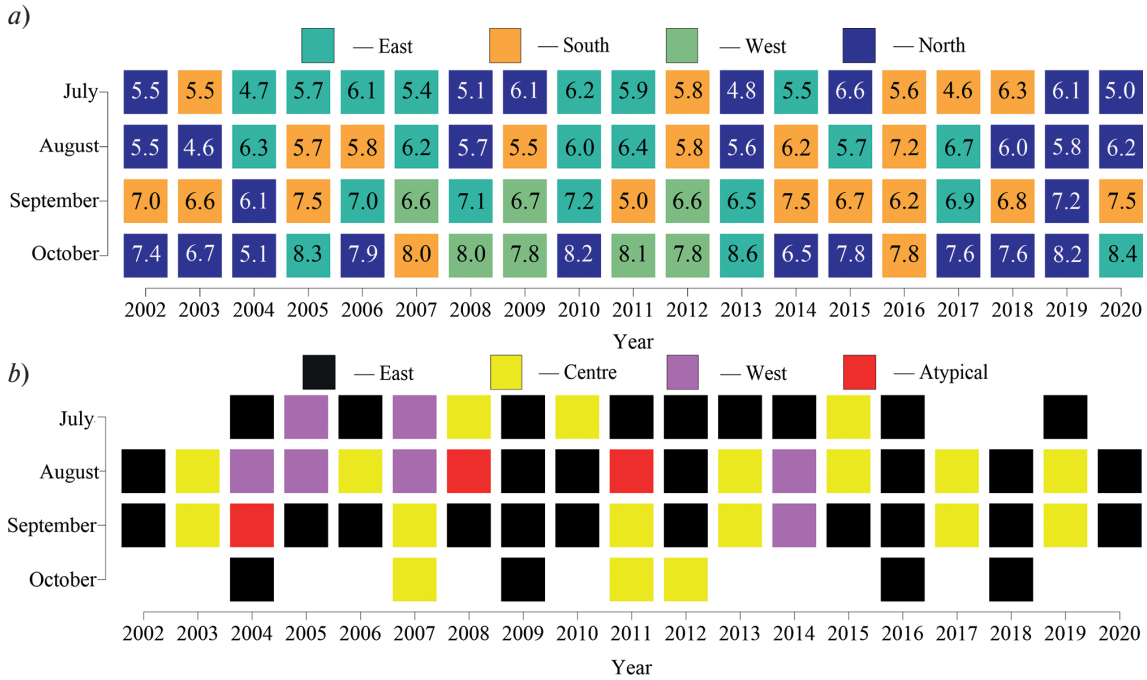

Fig. 10. Wind speed and direction (*a*), and types of RPFZ propagation (*b*) for the period from July to October from 2002 to 2020

In July, under the influence of the north wind, currents of the southeast direction arise in the near-surface layers of the sea. As a result, the RPFZ extends from the Yamal Peninsula to the northern tip of archipelago Novaya Zemlya. A similar pattern is observed in August, however, the RPFZ moves slightly southward and shifts to the center of the Kara Sea. In September, the wind speed increases, which enhances the influence of surface wind currents and entails a change in the position of the RPFZ, which is characterized by a shift of the zone towards the Siberian coast. The strengthening of southwestern winds against the background of negative air temperatures [15] and a significant decrease in river discharge in October (Table 4) leads to an even greater shift in the position of the RPFZ to the south towards the Siberian coast.

Comparison of the wind characteristics (Fig. 10, *a*) with the characteristics of the RPFZ area (Fig. 4, *b*) showed that during the periods of its maxima (2006–2007) a westerly wind with an average force of up to 6 m/s is observed, and minimums (2012, 2016) occur under the influence of southerly and eastern winds with an average speed of more than 6 m/s.

From Fig. 10, *b* it can be seen that the most common "eastern" type of the RPFZ propagation is observed during southern and southwestern winds with a speed of more than 6 m/s. This wind intensifies the movement of the lens of freshened waters along the Siberian coast, which is formed under the influence of the Coriolis force. The "central" type of the RPFZ is characterized by northerly winds with a speed of more than 6.5 m/s, the strength of which weakens the main geostrophic current along the coast. This leads to the displacement of the FSL to the west from the Siberian coast to the central part of the Kara Sea. A rare "western" type of the RPFZ propagation is formed by easterly winds with a speed of more than 6 m/s. It is likely that the increase in the Ekman transport shifts the surface cyclonic circulation in the central part of the Kara Sea [1], which leads to the deviation of the fresh water lens to the west. The conditions for the emergence of a "non-standard" type of the RPFZ propagation are characterized by the predominance of northern winds with a speed of just over 6 m/s. A small wind force weakens the Ekman transfer, which leads to the formation of extensive frontal zones, the separation of the waters of the internal lens of the FSL water into parts, and the formation of a "non-standard" type of the RPFZ propagation.

4.6. Influence of Atmospheric Circulation over Northern Eurasia on the Characteristics of the RPFZ

The Kara Sea is predominantly influenced by the polar climate [3]. As a result, the influence of air mass transfer processes associated with global atmospheric circulation on the climate of this sea is quite large [1]. The average indices SCAND (reflects zonal transport) and POL (reflects meridional transport) were involved in the analysis. The time course of the indices is shown in Fig. 11.

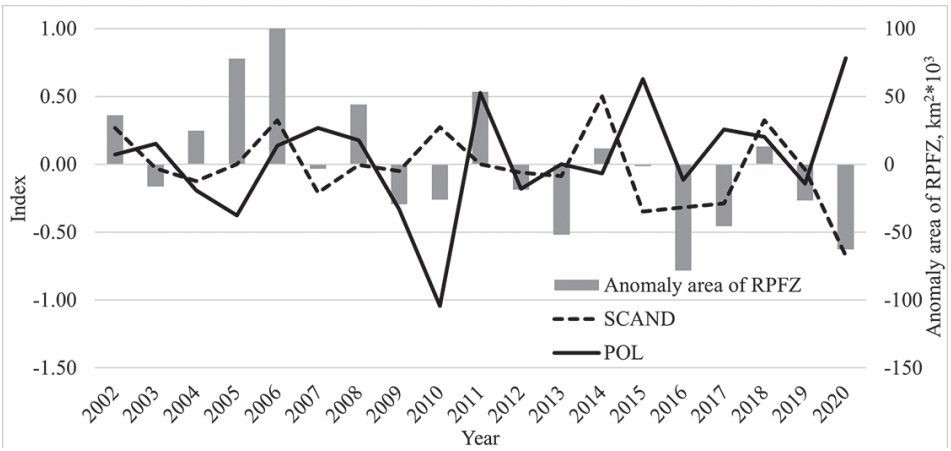

Fig. 11. Interannual dynamics of the averaged summer atmospheric circulation indices of the SCAND (dashed line), winter indices of the POL (solid line), and RPFZ anomalies (deviation from the average value for the entire study period, gray columns) of the area over the summer period

The variability of the SCAND fluctuations as a whole is characterized by negative values. The minimum value (–0.67) of the SCAND fluctuations is noted in 2020, and the maximum (0.18) in 2010. The average interannual amplitude is 0.9–1.0. Since 2019, a negative phase has been observed, which is reflected in the weakening of the zonal transport of warm Atlantic air and the processes of blocking cyclones passing from west to east. The variability of the POL index (black line) is mainly characterized by positive values. The minimum of the index (–1.04) is observed in 2010, and the maximum (0.78) in 2020. The range of interannual fluctuations is 1.8–2. Between 2019 and 2020 this index is characterized by a positive phase, which reflects an increase in the meridional transport of cold Arctic air from the Arctic and an increase in the number of passing cyclones from north to south.

Mutual analysis of the interannual variability of the RPFZ parameters and global atmospheric circulation indices showed that the large SST gradients in the RPFZ in 2010, 2016, and 2019 observed during the negative phase of the POL indices. Probably, against the background of the weakening of the meridional transport of cold air from the Arctic to Eurasia [29] cooling of sea waters intensifies, while river waters remain warm, which further affects the intensity of the SST gradient in the RPFZ. Minimum values of SST gradients in the RPFZ in 2010, 2018 and 2020 are registered with the growth of the SCAND indices. Most likely, this is due to the intensification of zonal atmospheric circulation [29], which increases the inflow of warm air from the Atlantic and minimizes the inhomogeneity of the SST gradient. The maximum values of the RPFZ area in 2006 correspond with the growth of both indices of atmospheric circulation. Minimum values of the RPFZ area in 2012 and 2016 registered in the negative phase with indices SCAND and POL. It is possible that a decrease in the intensity of global transport against the background of significant melting of the sea ice cover affected the intensity of water heating, which affected the area of the RPFZ.

The correlation analysis of the atmospheric circulation with the RPFZ parameters showed that there is a relationship between the summer SCAND index ($r = 0.65$) and the summer area of the RPFZ. A possible reason for this relationship is the enhancement of zonal transport [28], which affected the regional wind circulation that determines the distribution of surface waters of the RPFZ.

5. Conclusion

One of the most important results of this work is the obtained long-term estimates of the spatiotemporal variability and parameters of the RPFZ in the Kara Sea as a separate hydrological structure of waters.

For the first time for this region, when determining the physical and geographical characteristics of the RPFZ, a universal methodology was applied, which was based on the use of cluster analysis based on complex satellite remote sensing data. The method is quite simple to use and suitable for identifying frontal zones in various seas of the Arctic region.

The paper calculated and presented the average long-term and interannual quantitative characteristics of the surface manifestations of the RPFZ. The long-term SST gradient in the frontal zone over the entire study

period was 0.08 °C/km, SSS was 0.1 PSU/km, and the area was 155,000 km^2. The average long-term positions of the RPFZ in the warm period of the year were described. The variability of interannual estimates of the SST gradient in the RPFZ ranged from 0.03 to 0.17 °C/km, the SSS gradient from 0.06 to 0.19 PSU/km, and the area from 50,000 to 340,000 km^2. Significant anomalies of different signs were observed in almost all parameters of the RPFZ in the second decade of the 21st century. This is especially strongly reflected in the surface temperature gradients, which are, on average, twice as high as the background values. The temperature gradient of the surface of the RPFZ over the second decade of the 21st century has weakened by 0.04 °C/km, and its area for the same period on average decreased by 100,000 km^2. The results obtained indicate a significant variability of the RPFZ over the past 20 years against the background of global changes in the climate of the Arctic [32].

An analysis of correlation estimates showed the presence of statistically significant relationships between regional and global processes and the parameters of the RPFZ waters. It has been established that the greatest contribution to the variability of the quantitative characteristics of the RPFZ is made by the river discharge of the Yenisei and the characteristics of the sea ice cover (area and state). A large value of the SCAND index is reflected in an increase in the area in the RPFZ, which may be due to the blocking of zonal transport and an increase in precipitation in the catchment area of the Ob and Yenisei rivers in different periods of the year.

Thus, the results of a long-term analysis of the RPFZ in the Kara Sea over the first two decades of the 21st century showed that global climate changes affect the characteristics of the frontal zone. The identified features of the long-term variability of parameters may be typical for other Arctic rivers (Lena, Kolyma, Mackenzie). The following works will be aimed at studying the synoptic variability of the RPFZ and creating a model for predicting its parameters.

Funding

Data processing of the frontal zone characteristics was carried out within the framework of the RFBR grant No. 20–35–90053 postgraduate students. Comparison and analysis of the connection between the parameters of the frontal zones and regional and global processes was carried out as part of the State assignment Theme No. FMWE-2021–0014.

References

1. *Pavlov V.K.*, *Pfirman S.L.* Hydrographic structure and variability of the Kara Sea: Implications for pollutant distribution. *Deep Sea Research Part II: Topical Studies in Oceanography*. 1995, 42, 6, 1369–1390. doi:10.1016/0967–0645(95)00046–1
2. *Harms I.H.*, *Karcher M.J.* Modeling the seasonal variability of hydrography and circulation in the Kara Sea. *Journal of Geophysical Research: Oceans*. 1999, 104, C6, 13431–13448. doi:10.1029/1999jc900048
3. *Dobrovolsky A.D.*, *Zalogin B.S.* Seas of the USSR. *Moscow*, *MGU*, 1982. 192 p. (in Russian).
4. *Oziel L.*, *Sirven J.*, *Gascard J.-C.* The Barents Sea frontal zones and water masses variability (1980–2011). *Ocean Science*. 2016, 12, 1, 169–184. doi:10.5194/os-12–169–2016
5. *Barton B.I.*, *Lique C.*, *Lenn Y.-D.* Water mass properties derived from satellite observations in the Barents Sea. *Journal of Geophysical Research: Oceans*. 2020, 125, e2019JC015449. doi:10.1029/2019JC015449
6. *Bauch D.*, *Cherniavskaia E.* Water Mass Classification on a Highly Variable Arctic Shelf Region: Origin of Laptev Sea Water Masses and Implications for the Nutrient Budget. *Journal of Geophysical Research: Oceans*. 2018, 123, 3, 1896–1906. doi:10.1002/2017jc013524
7. *Osadchiev A.A.*, *Frey D.I.*, *Shchuka S.A.*, *Tilinina N.D.*, *Morozov E.G.*, *Zavialov P.O.* Structure of the freshened surface layer in the Kara Sea during ice-free periods. *Journal of Geophysical Research: Oceans*. 2020, 1–35. doi:10.1029/2020jc016486
8. *Zatsepin A.G.*, *Zavialov P.O.*, *Kremenetskiy V.V.*, *Poyarkov S.G.*, *Soloviev D.M.* Fresh surface layer in the Kara Sea. *Oceanology*. 2010, 50, 5, 643–656. doi:10.1134/S0001437010050024
9. *Zavialov P.O.*, *Izhitskiy A.S.*, *Osadchiev A.A.*, *Pelevin V.V.*, *Grabovskiy A.B.* The structure of thermohaline and bio-optical fields in the surface layer of the Kara Sea in September 2011. *Oceanology*. 2015, 55, 4, 461–471. doi:10.1134/s0001437015040177
10. *Kubryakov A.A.*, *Stanichny S.V.*, *Zatsepin A.G.* River plume dynamics in the Kara Sea from altimetry-based Lagrangian model, satellite salinity and chlorophyll data. *Remote Sensing of Environment*. 2016, 176, 177–187. doi:10.1016/j.rse.2016.01.020
11. *Polukhin A.A.* The role of river runoff in the Kara Sea surface layer acidification and carbonate system changes. *Environmental Research Letters*. 2019, 14, 105007. doi:10.1088/1748–9326/ab421

12. *Konik A.A.*, *Zimin A.V.*, *Atadzhanova O.A.*, *Pedchenko A.P.* Assessment of the variability of the river plums frontal zone in the Kara Sea on the basis of integration of satellite remote sensing data. *Sovremennye Problemy Distantsionnogo Zondirovaniya Zemli iz Kosmosa*. 2021, 18, 2, 241–250 (in Russian). doi:10.21046/2070-7401-2021-18-2-241-250
13. *Holmes R.M.*, *Peterson B.J.*, *Zulidov V.V.* et al. Nutrient chemistry of the Ob' and Yenisey Rivers, Siberia: Results from June 2000 expedition and evaluation of longterm data sets. *Marine Chemistry*. 2001, 75, 219–227. doi:10.1016/s0304–4203(01)00038-x
14. *Fedorov K.N.* The physical nature and structure of oceanic fronts. *Leningrad, Gidrometeoizdat,* 1983. 296 p. (in Russian).
15. *Atadzhanova O.A.*, *Zimin A.V.*, *Svergun E.I.*, *Konik A.A.* Submesoscale eddy structures and frontal dynamics in the Barents Sea. *Physical Oceanography*. 2018, 25, 3, 220–228. doi:10.22449/1573-160X-2018-3-220-228
16. *Zhuk V.R.*, *Kubryakov A.A.* Interannual variability of the Lena River plume propagation in 1993–2020 during the ice-free period on the base of satellite salinity, temperature, and altimetry measurements. *Remote Sensing*. 2021, 13, 21, 4252, 1–20. doi:10.3390/rs13214252
17. *Supply A.*, *Boutin J.*, *Vergely J.-L.*, *Kolodziejczyk N.*, *Reverdin G.*, *Reul N.*, *Tarasenko A.* New insights into SMOS sea surface salinity retrievals in the Arctic Ocean. *Remote Sensing of Environment*. 2020, 249, 112027. doi:10.1016/j.rse.2020.112027
18. *Janout M.A.* et al. Kara Sea freshwater transport through Vilkitsky Strait: Variability, forcing, and further pathways toward the western Arctic Ocean from a model and observations. *Journal of Geophysical Research: Oceans*. 2015, 120, 4925–4944. doi:10.1002/2014JC010635
19. *Glukhovets D.I.*, *Goldin Y.A.* Surface desalinated layer distribution in the Kara Sea determined by shipboard and satellite data. *Oceanologia*. 2020, 62, 364–373. doi:10.1016/j.oceano.2020.04.002
20. *Warner J.L.*, *Screen J.A.*, *Scaife A.A.* Links between Barents-Kara Sea ice and the extratropical atmospheric circulation explained by internal variability and tropical forcing. *Geophysical Research Letters*. 2019, 1–18. doi:10.1029/2019gl085679
21. *Kostianoy A.G.*, *Nihoul J.C.J.*, *Rodionov V.B.* Physical oceanography of the frontal zones in Sub-Arctic Seas. *Elsevier Oceanography Series*, 2004. 71 p.
22. *Ivshin V.A.*, *Trofimov A.G.*, *Titov O.V.* Barents Sea thermal frontal zones in 1960–2017: variability, weakening, shifting. *ICES Journal of Marine Science*. 2019, 76, i3—i9. doi:10.1093/icesjms/fsz159
23. *Liu Y.*, *Minnett P.J.* Sampling errors in satellite-derived infrared sea-surface temperatures. Part I: Global and regional MODIS fields. *Remote Sensing of Environment*. 2016, 177, 48–64. doi:10.1016/j.rse.2016.02.026
24. *Meissner T.*, *Wentz F.J.*, *and Le Vine D.M.* The salinity retrieval algorithms for the NASA Aquarius Version 5 and SMAP Version 3 releases. *Remote Sensing*. 2018, 10, 1121. doi:10.3390/rs10071121
25. *Ablain M.* et al. Improved sea level record over the satellite altimetry era (1993–2010) from the Climate Change Initiative project. *Ocean Science*. 2015, 11, 67–82. doi:10.5194/os-11–67–2015
26. *Spreen G.*, *Kaleschke L.*, *Heygster G.* Sea ice remote sensing using AMSR-E89-GHz channels. *Journal of Geophysical Research*. 2008, 113, C02S03. doi:10.1029/2005JC003384
27. Climate Diagnostics Bulletin. Climate Prediction Center. *US Department of Commerce*, 1999. 80 p.
28. *Barnston A.G.*, *Livezey R.E.* Classification, seasonality and persistence of low-frequency atmospheric circulation patterns. *Monthly Weather Review*. 1987, 115, 6, 1083–1126. doi:10.1175/1520–0493(1987)115<1083: csapol>2.0.co;
29. *Gao N.*, *Bueh C.*, *Xie Z.*, *Gong Y.A.* Novel identification of the Polar/Eurasia pattern and its weather impact in May. *Journal of Meteorological Research*. 2019, 33, 5, 810–825. doi:10.1007/s13351-019-9023-z
30. *Kuzin V.I.*, *Lapteva N.A.* Mathematical simulation of runoff of main Siberian rivers. *Atmospheric and Oceanic Optics*. 2014, 27, 6, 525–529.
31. *Karklin V.O.*, *Yulin A.V.*, *Sharatunova M.V.*, *Mochnova L.P.* Climate variability of the Kara Sea ice massifs. *Arctic and Antarctic Research*. 2017, 4, 37–46 (in Russian). doi:10.30758/0555-2648-2017-0-4-37-46
32. *Yamanouchi T.*, *Takata K.* Rapid change of the Arctic climate system and its global influences — Overview of GRENE Arctic climate change research project (2011–2016). *Polar Science*. 2020, 100548. doi:10.1016/j.polar.2020.100548

Литература

1. *Pavlov V.K.*, *Pfirman S.L.* Hydrographic structure and variability of the Kara Sea: Implications for pollutant distribution // Deep Sea Research Part II: Topical Studies in Oceanography. 1995. Vol. 42, N 6. P. 1369–1390. doi:10.1016/0967–0645(95)00046–1
2. *Harms I.H.*, *Karcher M.J.* Modeling the seasonal variability of hydrography and circulation in the Kara Sea // Journal of Geophysical Research: Oceans. 1999. Vol. 140, N C6. P. 13431–13448. doi:10.1029/1999jc900048

3. *Добровольский А.Д.*, *Залогин Б.С.* Моря СССР. М.: МГУ, 1982. 192 с.
4. *Oziel L.*, *Sirven J., Gascard J.-C.* The Barents Sea frontal zones and water masses variability (1980–2011) // Ocean Science. 2016. Vol. 12, N 1. P. 169–184. doi:10.5194/os-12–169–2016
5. *Barton B.I.*, *Lique C.*, *& Lenn Y.-D.* Water mass properties derived from satellite observations in the Barents Sea // Journal of Geophysical Research: Oceans. 2020. Vol. 125. e2019JC015449. doi:10.1029/2019JC015449
6. *Bauch D., Cherniavskaia E.* Water Mass Classification on a Highly Variable Arctic Shelf Region: Origin of Laptev Sea Water Masses and Implications for the Nutrient Budget // Journal of Geophysical Research: Oceans. 2018. Vol. 123, N 3. P. 1896–1906. doi:10.1002/2017jc013524
7. *Osadchiev A.A.*, *Frey D.I.*, *Shchuka S.A.*, *Tilinina N.D.*, *Morozov E.G.*, *Zavialov P.O.* Structure of the freshened surface layer in the Kara Sea during ice-free periods // Journal of Geophysical Research: Oceans. 2020. P. 1–35. doi:10.1029/2020jc016486
8. *Зацепин А.Г.*, *Завьялов П.О.*, *Кременецкий В.В.*, *Поярков С.Г., Соловьев Д.М.* Поверхностный опресненный слой в Карском море // Океанология. 2010. Т. 50, № 5. С. 698–708.
9. *Завьялов П.О.*, *Ижницкий А.С.*, *Осадчиев А.А.*, *Пелевин В.В.*, *Грабовский А.Б.* Структура термохалинных и биооптических полей на поверхности Карского моря осенью 2011 года // Океанология. 2015. Т. 55, № 4. С. 514. doi:10.7868/S0030157415040176
10. *Kubryakov A.A.*, *Stanichny S.V.*, *Zatsepin A.G.* River plume dynamics in the Kara Sea from altimetry-based Lagrangian model, satellite salinity and chlorophyll data // Remote Sensing of Environment. 2016. Vol. 176. P. 177–187. doi:10.1016/j.rse.2016.01.020
11. *Polukhin A.A.* The role of river runoff in the Kara Sea surface layer acidification and carbonate system changes // Environmental Research Letters. 2019. Vol. 14. P. 105007. doi:10.1088/1748–9326/ab421
12. *Коник А.А.*, *Зимин А.В.*, *Атаджанова О.А.*, *Педченко А.П.* Оценка изменчивости характеристик Стоковой фронтальной зоны Карского моря на основе комплексирования данных спутникового дистанционного зондирования // Современные проблемы дистанционного зондирования Земли из космоса. 2021. Т. 18, № 2. С. 241–250. doi:10.21046/2070-7401-2021-18-2-241-250
13. *Holmes R.M.*, *Peterson B.J.*, *Zulidov V.V.* et al. Nutrient chemistry of the Ob' and Yenisey Rivers, Siberia: Results from June 2000 expedition and evaluation of longterm data sets // Marine Chemistry. 2001. Vol. 75. P. 219–227. doi:10.1016/s0304–4203(01)00038-x
14. *Федоров К.Н.* Физическая природа и структура океанических фронтов. Л.: Гидрометеоиздат, 1983. 296 с.
15. *Атаджанова О.А.*, *Зимин А.В.*, *Свергун Е.И.*, *Коник А.А.* Субмезомасштабные вихревые структуры и фронтальная динамика в Баренцевом море // Морской гидрофизический журнал. 2018. Т. 34, № 3. С. 237–246. doi:10.22449/0233-7584-2018-3-237-246
16. *Zhuk V.R.*, *Kubryakov A.A.* Interannual variability of the Lena River plume propagation in 1993–2020 during the ice-free period on the base of satellite salinity, temperature, and altimetry measurements // Remote Sensing. 2021. Vol. 13, N 21. 4252. P. 1–20. doi: 10.3390/rs13214252
17. *Supply A., Boutin J.*, *Vergely J.-L., Kolodziejczyk N.*, *Reverdin G.*, *Reul N.*, *Tarasenko A.* New insights into SMOS sea surface salinity retrievals in the Arctic Ocean // Remote Sensing of Environment. 2020. Vol. 249. P. 112027. doi:10.1016/j.rse.2020.112027
18. *Janout M.A.*, et al. Kara Sea freshwater transport through Vilkitsky Strait: Variability, forcing, and further pathways toward the western Arctic Ocean from a model and observations // Journal of Geophysical Research: Oceans. 2015. Vol. 120. P. 4925–4944. doi:10.1002/2014JC010635
19. *Glukhovets D.I.*, *Goldin Y.A.* Surface desalinated layer distribution in the Kara Sea determined by shipboard and satellite data // Oceanologia. 2020. Vol. 62. P. 364–373. doi:10.1016/j.oceano.2020.04.002
20. *Warner J.L.*, *Screen J.A.*, *Scaife A.A.* Links between Barents-Kara Sea ice and the extratropical atmospheric circulation explained by internal variability and tropical forcing // Geophysical Research Letters. 2019. P. 1–18. doi:10.1029/2019gl085679
21. *Kostianoy A.G.*, *Nihoul J.C.J.*, *Rodionov V.B.* Physical oceanography of the frontal zones in Sub-Arctic Seas. Elsevier Oceanography Series, 2004. 71 p.
22. *Ivshin V.A.*, *Trofimov A.G.*, *Titov O.V.* Barents Sea thermal frontal zones in 1960–2017: variability, weakening, shifting // ICES Journal of Marine Science. 2019. Vol. 76. P. i3—i9. doi:10.1093/icesjms/fsz159
23. *Liu Y.*, *Minnett P.J.* Sampling errors in satellite-derived infrared sea-surface temperatures. Part I: Global and regional MODIS fields // Remote Sensing of Environment. 2016. Vol. 177. P. 48–64. doi:10.1016/j.rse.2016.02.026
24. *Meissner T.*, *Wentz F.J.*, *Le Vine D.M.* The Salinity Retrieval Algorithms for the NASA Aquarius Version 5 and SMAP Version 3 Releases // Remote Sensing. 2018. Vol. 10. P. 1121. doi:10.3390/rs10071121

25. *Ablain M.* et al. Improved sea level record over the satellite altimetry era (1993–2010) from the Climate Change Initiative project // Ocean Science. 2015. Vol. 11. P. 67–82. doi:10.5194/os-11–67–2015
26. *Spreen G.*, *Kaleschke L.*, *Heygster G.* Sea ice remote sensing using AMSR-E89-GHz channels // Journal of Geophysical Research. 2008. Vol. 113. P. C02S03. doi:10.1029/2005JC003384
27. Climate Diagnostics Bulletin. Climate Prediction Center. US Department of Commerce, 1999. 80 p.
28. *Barnston A.G.*, *Livezey R.E.* Classification, seasonality and persistence of low-frequency atmospheric circulation patterns // Monthly Weather Review. 1987. Vol. 115, N 6. P. 1083–1126. doi:10.1175/1520–0493(1987)115<1083:csapol>2.0.co;
29. *Gao N.*, *Bueh C.*, *Xie Z.*, *Gong Y.A.* Novel Identification of the Polar/Eurasia Pattern and Its Weather Impact in May // Journal of Meteorological Research. 2019. Vol. 33, N 5. P. 810–825. doi:10.1007/s13351–019–9023-z
30. *Кузин В.И.*, *Лаптева Н.А.* Математическое моделирование стока основных рек Сибири // Оптика атмосферы и океана. 2014. Т. 27, № 6. С. 525–529.
31. *Карклин В.П.*, *Юлин А.В.*, *Шаратунова М.В.*, *Мочнова Л.П.* Климатическая изменчивость ледяных массивов Карского моря // Проблемы Арктики и Антарктики. 2017. № 4. С. 37–46. doi:10.30758/0555-2648-2017-0-4-37-46
32. *Yamanouchi T.*, *Takata K.* Rapid change of the Arctic Climate system and its global influences — Overview of GRENE Arctic Climate change research project (2011–2016) // Polar Science. 2020. P. 100548. doi:10.1016/j.polar.2020.100548

About the Authors

Aleksandr A. Konik, РИНЦ AuthorID: 950834, ORCID: 0000-0002-2089-158X, Scopus AuthorID: 57203864647, e-mail: konikrshu@gmail.com

Alexey V. Zimin, РИНЦ AuthorID: 124451, ORCID: 0000-0003-1662-6385, Scopus AuthorID: 55032301400, WoS ResearcherID: C-5885-2014, e-mail: zimin2@mail.ru

Oksana A. Atadzhanova, РИНЦ AuthorID: 846708, ORCID: 0000-0001-6820-0533, e-mail: oksana.atadzhanova@gmail.com